

# Four Shades of Brown: Tuning of Electrochromic Polymer Blends Toward High-Contrast Eyewear

Anna M. Österholm,<sup>\*,†</sup> D. Eric Shen,<sup>†,‡</sup> Justin A. Kerszulis,<sup>†</sup> Rayford H. Bulloch,<sup>†</sup> Michael Kuepfert,<sup>§</sup> Aubrey L. Dyer,<sup>||</sup> and John R. Reynolds<sup>\*,†</sup>

<sup>†</sup>School of Chemistry and Biochemistry, School of Materials Science and Engineering, Center for Organic Photonics and Electronics, Georgia Institute of Technology, Atlanta, Georgia 30332, United States

<sup>‡</sup>BASF-SE c/o InnovationLab GmbH, Heidelberg 69115, Germany

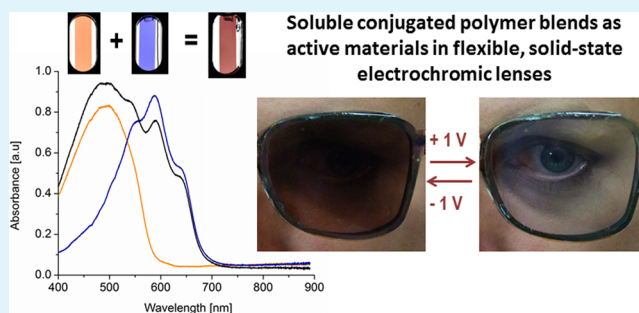
<sup>§</sup>Re-synthesis Laboratory, NC/IS, BASF Corporation, Tarrytown, New York 10591, United States

<sup>||</sup>Department of Natural Sciences, Clayton State University, Morrow, Georgia 30260, United States

## S Supporting Information

**ABSTRACT:** We report a straightforward strategy of accessing a wide variety of colors through simple predictive color mixing of electrochromic polymers (ECPs). We have created a set of brown ECP blends that can be incorporated as the active material in user-controlled electrochromic eyewear. Color mixing of ECPs proceeds in a subtractive fashion, and we acquire various hues of brown through the mixing of cyan and yellow primaries in combination with orange and periwinkle-blue secondary colors. Upon oxidation, all of the created blends exhibit a change in transmittance from ca. 10 to 70% in a few seconds. We demonstrate the attractiveness of these ECP blends as active materials in electrochromic eyewear by assembling user-controlled, high-contrast, fast-switching, and fully solution-processable electrochromic lenses with colorless transmissive states and colored states that correspond to commercially available sunglasses. The lenses were fabricated using a combination of inkjet printing and blade-coating to illustrate the feasibility of using soluble ECPs for high-throughput and large-scale processing.

**KEYWORDS:** electrochromic polymers, dioxothiophenes, color mixing, electrochromic eyewear, electrochromic devices, organic electronics



## INTRODUCTION

Electrochromics for user-controlled smart wearable electronics target diverse markets, ranging from electrochromic fabrics and lenses for consumer fashion, to military camouflage and visors that require rapid response adaptive technology. In the field of color changing eyewear, the most widespread products are photochromic lenses, which reversibly change between colored states in response to changes in light. These glasses can either transition between a lighter shade and a darker shade while maintaining their color, or switch from one color in low light conditions to a different color in bright light conditions.<sup>1–4</sup> The majority of photochromic lenses are passively activated by UV light, which means that the color transition cannot occur indoors or while driving. The active materials used in photochromic eyewear are evaluated on metrics such as their color in each state, the change in transmittance ( $\Delta\%T$ ) upon switching, and the rate at which they switch between states, to name a few. Commercially available photochromic eyewear, often based on compounds such as silver halides, have  $\Delta\%T$  of 18–60% depending on the color of the lens.<sup>1–3</sup> The  $\Delta\%T$  and the switching time of these lenses depend either on the light

intensity, the temperature, or a combination of the two. Typically, the clear-to-colored (light-to-dark) transition is faster and occurs in 10–60 s, whereas the colored-to-clear transition can take up to several minutes.<sup>1–3</sup> For certain users (pilots, urban security, drivers, etc.), a more rapid response time, as well as the ability for the transmittance change to be user-controlled, is expected to be highly advantageous, if not crucial.

An alternative to photochromic compounds and a route toward fully user-controlled eyewear is to use electrochromic polymers (ECPs). These polymers possess many properties attractive to eyewear applications, with performance on par with or even superior to commercially available products. One attractive feature of the current eyewear market is the range of lens colors. With regard to ECPs, the entire color palette has been completed using solution-processable, cathodically coloring ECPs that can switch to a highly transmissive state upon oxidation, all within a small voltage window.<sup>5</sup> In addition to

**Received:** October 13, 2014

**Accepted:** December 19, 2014

**Published:** January 9, 2015

these vibrantly colored ECPs, a broadly absorbing black-to-transmissive polymer has also been developed that exhibits a  $\Delta T$  of 48% (at 555 nm) with a highly transmissive and achromatic oxidized state.<sup>6,7</sup> Another important metric of eyewear is stability to irradiation and environmental stress. Weathering studies have demonstrated that when electrochromic devices (ECDs) are constructed in a glovebox using a sealant, or when encapsulated with a barrier layer, device stabilities are sufficient for a range of applications.<sup>8,9</sup> In addition to these properties, ECPs complete a full switch on a much faster time scale of seconds or less with transmittance changes on the order of 50–70%.<sup>5</sup> In spite of these promising results, few studies have developed ECDs beyond simple and small window-type devices. Some noteworthy examples of more recent developments of ECP-based transmissive ECDs include lenses/goggles,<sup>10–12</sup> self-powered and energy harvesting EC/photovoltaic devices,<sup>13,14</sup> ECDs with active areas exceeding 100 cm<sup>2</sup>,<sup>15</sup> continuous and roll-to-roll compatible fabrication of ECDs,<sup>16</sup> color mixing using dual-active ECDs,<sup>17,18</sup> and all-printed passive matrix addressed ECDs,<sup>19</sup> to name a few. The few examples of electrochromic lenses currently found in the literature<sup>10–12,20</sup> are blue in their colored states and tend to use electrochemical polymerization to deposit the active layer instead of a roll-to-roll compatible solution-processing method. To address this deficiency, we have sought to demonstrate the attractiveness of ECPs by assembling fully user-controlled, high-contrast, fast-switching, and solution-processable electrochromic lenses with colorless transmissive states and colored states that correspond to commercially available sunglasses.

Many sunglasses are available in a variety of shades of brown, ranging from reddish-browns, to greenish-browns, to amber-browns. To demonstrate the versatility of employing ECPs to envelope the color space, we have developed a set of fast-switching, brown ECP blends that exhibit  $\Delta T$  of >60% between their colored and bleached states. Traditionally, we have utilized simple side-chain modification of a polymer backbone to either electronically or sterically tune the coloration of a material.<sup>5,21,22</sup> However, given the large library of colors at our disposal, as well as the tertiary nature of brown, which is inherently a combination of multiple colors, we demonstrate here the straightforward strategy of accessing a wide variety of brown hues through simple predictive color mixing. In particular, color mixing of ECPs proceeds in a subtractive fashion, and we acquire various hues through the mixing of cyan and yellow primaries in combination with orange and periwinkle-blue secondary colors to illustrate the concept. As such, using only a small handful of starting ECPs, virtually any color of interest can be achieved that would display the correspondingly high contrasts and rapid switching times of its blend components, assuming that all components are soluble in the same solvent system. The ability to predictably blend ECPs while retaining the performance of the blend components should broaden the scope of these polymers, not just for the development of electrochromic sunglasses and visors, but also for electrochromic window and signage applications.

## EXPERIMENTAL SECTION

**Materials.** ECP-Orange<sup>23</sup> (oxidative polymerization;  $M_n$ : 249 kDa; PDI: 2.4), and ECP-Cyan<sup>24</sup> (direct arylation;  $M_n$ : 53 kDa; PDI: 1.7) were synthesized via previously reported methodologies. The syntheses of ECP-Yellow ( $M_n$ : 226 kDa; PDI: 1.9) and ECP-Periwinkle ( $M_n$ : 77.8 kDa; PDI: 3.4) using previously optimized direct

arylation conditions<sup>24</sup> are described in more detail in the Supporting Information (Scheme S1, Figures S1–S3). Toluene (Fisher Scientific, 99.5%) and chloroform (BDH, 99.8%) were used without further purification to dissolve the ECPs. Propylene carbonate (PC, 99.5%) was purchased from Acros Organics and purified using a solvent purification system from Vacuum Atmospheres. Tetrabutylammonium hexafluorophosphate (TBAPF<sub>6</sub>, 98%, Alfa Aesar) was purified by recrystallizing from ethanol and then dissolved in PC at a 0.5 M concentration. ITO coated glass slides (25 × 75 × 0.7 mm<sup>3</sup>, sheet resistance 8–12  $\Omega$ /sq) were purchased from Delta Technologies, Ltd., and cleaned with toluene, acetone, and isopropanol. ECP solutions (conc. 2–5 mg/mL) were made using a 1:1 (v/v) toluene/chloroform mixture. For the film characterization, the polymers were deposited (to an optical density of 1 au at  $\lambda_{\max}$  over an area of 2.1 cm<sup>2</sup>) on ITO via spray casting using an Iwata-Eclipse HP-BC airbrush with an optimized argon pressure of approximately 12 psi.

**ECP-Blends and Absorption Coefficients.** When making the ECP blends, we used absorption coefficients to determine the proper ratios of ECPs to blend to obtain the desired shades of brown. During ECP blending, the weight ratio of the components does not reflect the ratio of their composite spectra. Rather, their spectra originate not from a discrete chromophore but from a distribution of chromophores whose lengths cannot be readily determined. Therefore, it is more reasonable to calculate a bulk property like film absorptivity. With this value, ratios of absorptivity can be adjusted to more accurately arrive at the desired color.

The absorption coefficients were determined by spraying the evaluated ECPs to a range of optical densities (approximately 0.3 to 2 a.u.), plotting film absorption at  $\lambda_{\max}$  as a function of film thickness or film volume (film thickness multiplied by the area of the spectrophotometer beam), and taking the slope to be the absorption coefficient. An example using ECP-Orange is shown in Figure S4 (Supporting Information). Throughout this manuscript the blend ratios reported are based on these absorption coefficients. Of the ECP components used to make the reported brown blends, ECP-Cyan has the highest absorption coefficient of 0.0088 nm<sup>-1</sup>, followed by ECP-Yellow with a 0.0060 nm<sup>-1</sup> absorption coefficient. ECP-Orange and ECP-Periwinkle have similar absorption coefficients, 0.0044 and 0.0045, respectively. For all the ECPs, the absorption spectra used for the absorption coefficient determinations were of films that had been electrochemically conditioned by cyclic voltammetry (–0.8 to 0.8 V at 50 mV/s for 5 cycles) before recording the spectra as some ECPs change spectral and color properties after coming into contact with electrolyte solution during redox switching.<sup>25</sup> ECP-Periwinkle, for example, has a purple color in the as-cast state whereas the switched film has a red-shifted  $\lambda_{\max}$  that gives rise to the periwinkle-blue color. This is illustrated in Figure S5 (Supporting Information) for a Yellow–Periwinkle blend, where the spectrum of an as-cast film is compared with the spectrum of the same film that has been electrochemically conditioned as described above. The ECP-Yellow component with a  $\lambda_{\max}$  at 450 nm displays no changes upon electrochemical conditioning whereas the ECP-Periwinkle component ( $\lambda_{\max}$  at ca. 600 nm) changes significantly, with the onset of absorption red-shifting by approximately 50 nm.

**Film Characterization.** Electrochemical measurements were performed in a three-electrode cell with a coiled Pt wire as the counter electrode, a Ag/Ag<sup>+</sup> (10 mM AgNO<sub>3</sub> in 0.5 M TBAPF<sub>6</sub>-ACN,  $E_{1/2}$  for ferrocene: +85 mV), and ECP-coated ITO as the working electrode. The voltage was controlled using an EG&G PAR 273A potentiostat/galvanostat under CorrWare control. All films were electrochemically conditioned by cyclic voltammetry (–0.8 V and +0.8 V at 50 mV/s for 5 cycles) before recording spectra. The switching speed of the blends was determined by square wave potential step absorptiometry. The in situ spectroscopic analyses were performed using an Ocean Optics USB2000+ fiber-optic spectrophotometer. The absorbance and transmittance data for the film measurements are subtracted for substrate absorption. The colors of the ECP components and the ECP blends were quantified by converting the absorbance spectra to CIELAB L\*a\*b\* color coordinates where the L\* represents the white–black balance (in essence the lightness or

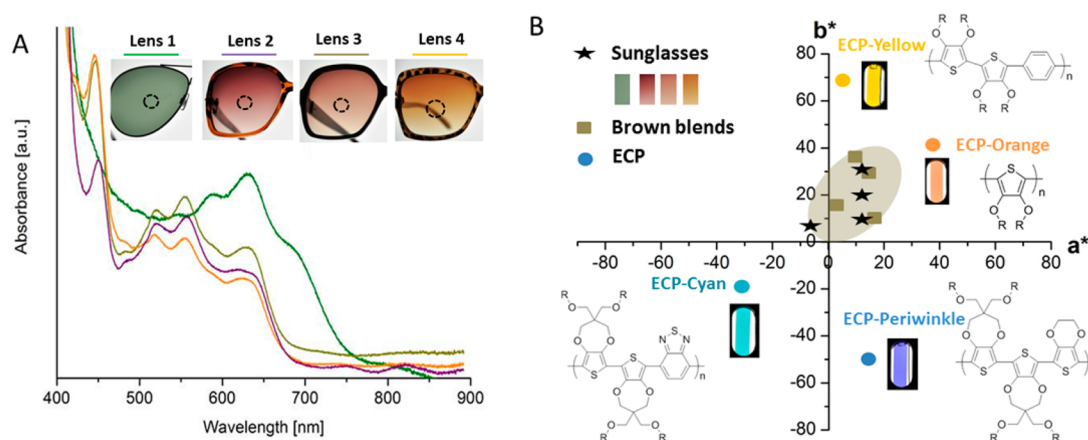


**Figure 1.** (A) Absorption spectra and photographs of the four commercial sunglass lenses, the circles in the photographs indicate the area of the lens from which the spectra were recorded; (B)  $a^*b^*$  plot showing the color coordinates for the lenses (★), the evaluated ECPs used for color mixing (●, R = 2-ethylhexyl), and the four brown blends (■) that will be discussed in greater detail below.

darkness of a color),  $a^*$  represents the green–red balance, and  $b^*$  represents the blue–yellow balance of a given color.<sup>26</sup> Photography was performed in a light booth with D50 illumination using a Nikon D90 SLR camera with a Nikon 18–105 mm VR lens. The photographs are presented without any manipulation apart from photograph cropping. The degree of color saturation (i.e., the intensity of a color expressed as the degree to which it differs from white) for the different blends was estimated using Equation (1)<sup>18</sup> where the color saturation ( $S_{ab}$ ) is defined as a ratio of chromatic color ( $C_{ab}^*$ , i.e., the hue of a color) to the total color sensation on a scale of 0–100, where 0 is gray and 100 is a pure color.

$$S_{ab} = \frac{C_{ab}^*}{\sqrt{C_{ab}^{*2} + L^{*2}}} 100\% = \frac{\sqrt{a^{*2} + b^{*2}}}{\sqrt{C_{ab}^{*2} + L^{*2}}} 100\% \quad (1)$$

**Device Assembly and Characterization.** Electrochromic lenses were fabricated in a 5-layer device stack consisting of a film of the 1.5:1 Orange–Periwinkle blend as the active layer, a UV-curable electrolyte, a film of 3,4-propylenedioxyppyrole-based minimally color changing polymer (MCCP)<sup>27</sup> as a charge storage layer, and PET/ITO as electrodes (sheet resistance approximately 100  $\Omega$ /sq). The PET/ITO foil was cleaned using toluene, acetone, and isopropanol and then air-dried. Silver contacts (3 mm in thickness, acquired from Sigma-Aldrich) patterned as the outlines of lenses were inkjet printed onto the PET/ITO using a Dimatix DMP2800, followed by drying in an oven at 130 °C for 30 min. MCCP (40 mg/mL in xylenes) and the ECP-blend, consisting of 20 mg/mL ECP-Orange and 13.3 mg/mL ECP-Periwinkle in chloroform/toluene/xylenes, were blade coated in a cleanroom environment to a desired thickness using a Zehntner blade coater with a blade gap of 50  $\mu$ m and a coating speed of 15 mm/sec. Xylenes were added to the solvent mixture to improve the film quality of the blade-coated films. Before assembling the lens, the MCCP layer was electrochemically oxidized at 0.4 V vs Ag/Ag<sup>+</sup> in 0.5 M lithium trifluoromethanesulfonate in PC. The UV curable electrolyte (approximately 200  $\mu$ m in thickness) was deposited onto one of the films and sandwiched between the two electrodes. The lens was then UV-cured ( $\lambda$ : 365 nm) for 1 min. The electrochromic lens was electrochemically switched using a WaveNow portable potentiostat and characterized using an Avantes spectrophotometer between 350 and 800 nm. The absorbance and transmittance data were obtained relative to air.

## RESULTS AND DISCUSSION

To define a range of colors to target, we selected the spectra (Figure 1A) of four commercial sunglasses (one green and three brown pairs, represented by stars in Figure 1B). These spectra can be converted to CIELAB ( $L^*a^*b^*$ ) colorimetric

coordinates, and plotted as shown in Figure 1B. Lenses 2, 3, and 4 that are in shades of brown have color coordinates in the  $+a^*$  and  $+b^*$  quadrants, whereas the green lens 1 is in the  $-a^*$  and  $+b^*$  quadrant. Based on the color coordinates for the different lenses, we defined an area in the  $a^*b^*$  color space that would give us hues that are comparable to commercially available eyewear. Lenses 2, 3, and 4 have absorbances ranging from 2 to 0.5 au (at 550 nm) across the lens. The difference in absorbance across one lens mainly translates into differences in  $L^*$ , though there are also some variation in  $a^*$  and  $b^*$  as shown in Table 1. Lens 1, on the other hand, has an even color and

**Table 1.**  $L^*a^*b^*$  Values for the Sunglass Lenses

lens	$L^*$	$a^*$	$b^*$	$S_{ab}$
1 (green)	47	−7	9	24
2 (purple-brown)	22–71	8–21	10–11	50–32
3 (reddish-brown)	37–71	5–16	17	43–31
4 (amber-brown)	37–73	4–18	28–34	61–47

absorbance across the entire lens. As we will show, this part of the color space can be recreated by preparing mixed blends consisting of just two or three ECPs. The color coordinates of the four ECP blends, as well as the coordinates of the ECP components used in the blends (ECP-Yellow, ECP-Orange, ECP-Cyan, and ECP-Periwinkle), are represented by squares and circles, respectively, in Figure 1B.

**ECP Components—Color and Contrast.** As mentioned, our group has developed a large library of ECPs spanning the entire color palette.<sup>5</sup> When mixing two ECPs, the color coordinate of the blend will lie somewhere between the coordinates of the component ECPs, depending on the ratio of the components. Tuning this ratio leads to a range of colors, approximated by the colors that lie along a line connecting the components. In selecting components for the brown blends, we chose ECPs so that weighted averages of their  $a^*$  and  $b^*$  values fell within the brown region defined in Figure 1B, narrowing down the ECPs for consideration. Additionally, the absorption coefficient of each component was used to determine the ratio required to obtain the desired hue. Among the ECPs we have synthesized, ECP-Orange and ECP-Cyan have averaged  $a^*b^*$  values that lie within the brown region defined in Figure 1B. ECP-Yellow is an alternative high-energy light absorber that can be used to create broadly absorbing blends. Here, we have

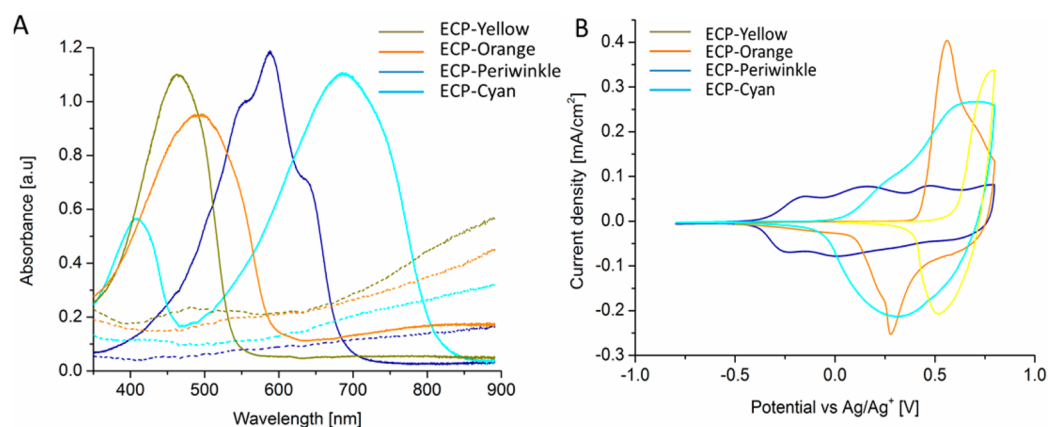


**Figure 2.** (A) Absorption spectra of ECP-Yellow (yellow lines), ECP-Orange (orange lines), ECP-Periwinkle (blue lines), and ECP-Cyan (cyan lines) in their oxidized (dashed lines) and charge neutral states (solid lines) on ITO/glass. (B) Cyclic voltammograms of ECP-Yellow (yellow line), ECP-Orange (orange line), ECP-Periwinkle (blue line), and ECP-Cyan (cyan line) recorded in 0.5 M TBAPF<sub>6</sub>-PC at 50 mV/s.

developed a new ECP-Yellow that has a higher  $\Delta\%T$  and a significantly lower oxidation potential than our previously reported yellow ECPs,<sup>28,29</sup> minimizing the risk of overoxidizing the low-energy light absorbing blend component. Blending ECP-Yellow with a blue ECP will also result in averaged  $a^*b^*$  values that fall in the defined brown region. The blue ECP used in this study is an all-donor ECP, referred to here as ECP-Periwinkle, that exhibits a 78%  $\Delta T$ , which is an improvement compared to the donor–acceptor ECP-Blue previously reported by our group.<sup>30,31</sup> In addition to its high  $\Delta T$ , ECP-Periwinkle in its electrochemically conditioned and charge neutral state has an absorption onset that perfectly matches that of lenses 2, 3, and 4, as shown in Figure S6 (Supporting Information). In this study, both ECP-Yellow and ECP-Orange were evaluated as the high-energy absorbers in conjunction with ECP-Periwinkle to cover both the low and high  $a^*$  boundaries of the brown region in Figure 1B.

The neutral and oxidized spectra of ECP-Orange, ECP-Periwinkle, ECP-Cyan, and our new ECP-Yellow are shown in Figure 2A. ECP-Periwinkle has the highest  $\Delta\%T$  (78%) at  $\lambda_{\max}$  of these four ECPs as a result of its highly transmissive oxidized state. ECP-Periwinkle also has the lowest oxidation potential of the evaluated ECPs, as shown in Figure 2B, and a fully transmissive state is reached at 0 V vs Ag/Ag<sup>+</sup>. ECP-Yellow has the highest oxidation potential requiring 0.7 V to achieve a highly transmissive and colorless state. ECP-Orange and ECP-Cyan have rather similar oxidation potentials, and at 0.5 V, both ECPs are in their fully oxidized states. Aside from  $\Delta\%T$  and oxidation potential, another important parameter is the switching speeds of the different ECPs. Chronoabsorptometry plots ( $\%T$  at  $\lambda_{\max}$ ; Figure S7, Supporting Information) were recorded by applying a potential square wave between  $-0.8$  and  $0.8$  V for 60, 30, 10, 5, 2, and 1 s. ECP-Orange takes the longest time to fully switch between the colored and the colorless states with a switching time on the order of 5 s using this experimental setup.<sup>23</sup> ECP-Yellow, ECP-Cyan, and ECP-Periwinkle all exhibit subsecond switching times.

**ECP Blends—Color and Contrast.** Color saturation relates color values ( $a^*$  and  $b^*$ ) to the color luminance ( $L^*$ ), which is the total light passed through a sample relative to a white standard. A high saturation ( $S_{ab}$ ) gives a vivid and intense color stimulus, whereas low saturation will appear more muted. Colors possessing broad absorbance spectra, such as browns, inherently possess low luminance and saturation. On the other

hand, colors possessing narrower absorbance spectra, such as our primary ECPs, have a high degree of color saturation, as shown in Table 2. In addition to spectral broadness, the

**Table 2. Color Coordinates and Color Saturation of the ECPs and ECP Blends (at 1.0 a.u.)**

ECP/ECP-blend	$L^*$	$a^*$	$b^*$	$S_{ab}$
yellow	87	10	80	92
orange	72	37	38	60
periwinkle	50	20	−49	72
cyan	69	−32	−18	53
1.5:1 orange–periwinkle	55	19	9	35
1.2:1 yellow–periwinkle	57	3	15	26
1.3:1:1 yellow–orange–periwinkle	57	15	30	47
1:1 orange–cyan	65	12	35	50

wavelength range of the dominant absorption also affects the  $S_{ab}$ . While the component ECPs themselves have high color saturation, blends will naturally possess broader spectra, which translate into a lower  $S_{ab}$  for the brown materials studied here.

To reproduce the color of lens 2 and achieve a shade of brown that represented the high  $a^*$  and low  $b^*$  range of the targeted color region, we set out to make an Orange–Periwinkle blend. ECP-Periwinkle and ECP-Orange have nearly identical absorption coefficients, which enables us to assume that if mixed in a 1:1 weight ratio, the two components should contribute equally to the blend color. From the values shown in Table 2 and Figure 1B, this would lead to an expected  $a^*$  value of ca. 30 and a  $b^*$  of ca.  $-5$  (i.e., outside the targeted color range due to the low  $b^*$ ). By increasing the ratio to 1.5:1 Orange–Periwinkle, we were able to tune the color and raise the  $b^*$  creating a blend that at 1 au had an  $L^*$  of 55,  $a^*$  of 19, and a  $b^*$  of 9, and a  $S_{ab}$  of 35, a close match to the color coordinates of lens 2. The spectra and photographs of this blend (in its neutral and oxidized states) compared against lens 2 are shown in Figure 3A. In addition to being a close spectral match to lens 2, this blend has a highly achromatic colorless state ( $L^*$  89,  $a^*$   $-1.7$ ,  $b^*$   $-5$ ) with an average  $\Delta\%T$  of 66% at 500 nm ( $\lambda_{\max}$ ) between the colored and the colorless states as shown in Figure S8A (Supporting Information).

To create a brown shade that covers the low  $a^*$  side of the targeted color range, we blended ECP-Yellow with ECP-Periwinkle. An advantage of this blend over the Orange–

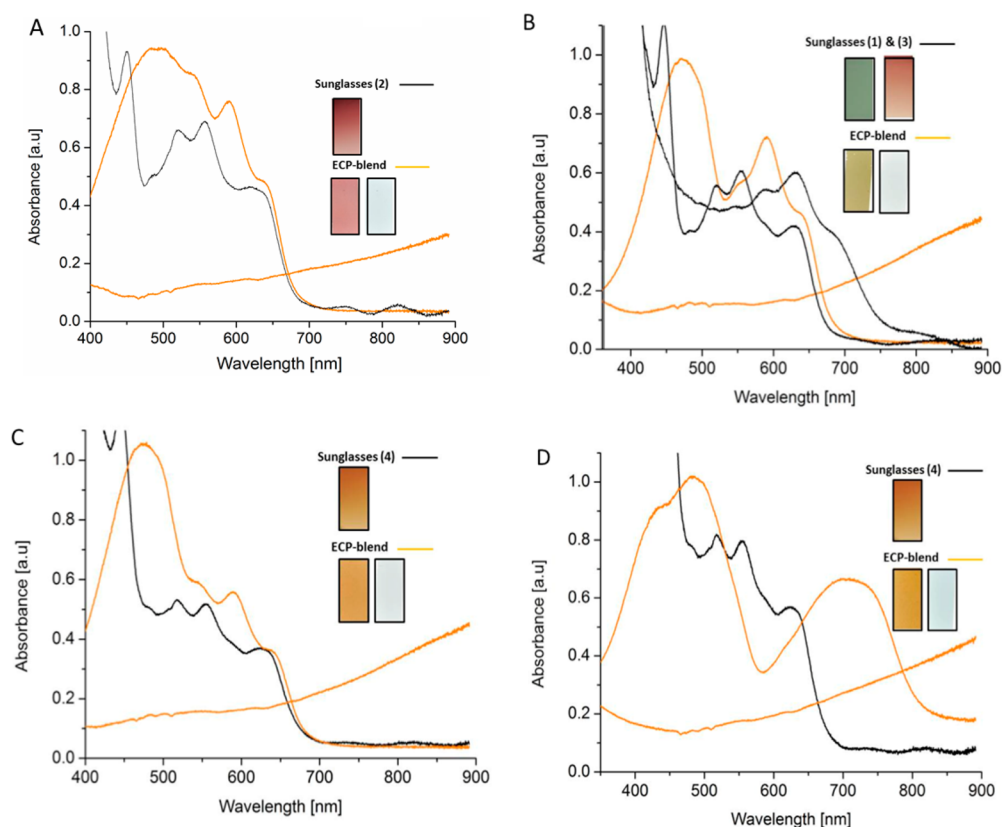


**Figure 3.** Spectra (in neutral and oxidized states) and photographs of (A) the 1.5:1 Orange–Periwinkle blend, (B) the 1.2:1 Yellow–Periwinkle blend, (C) the 1.3:1:1 Yellow–Orange–Periwinkle blend, and (D) the 1:1 Orange–Cyan blend. The spectra and photographs of the sunglass lens that is the closest match for each blend are also shown in the respective figures.

Periwinkle blend is the intuitive effect that varying the component ratios has on the  $a^*b^*$  values of the blend. In the Yellow–Periwinkle blend, varying the amounts of ECP–Yellow predominantly alters the  $b^*$  value, or the yellowness, of the blend. In contrast, in the Orange–Periwinkle blend, changing the amounts of either component leads to notable changes in both  $a^*$  and  $b^*$  values simultaneously because both Orange and Periwinkle have a sizable  $a^*$  and  $b^*$  component to their color. Figure 3B shows the spectra and photographs of one example of a Yellow–Periwinkle blend (1.2:1 blend,  $L^* 57$ ,  $a^* 3$ ,  $b^* 15$ ) compared to lens 1 and lens 3. The yellow and periwinkle ECPs have little spectral overlap between 550 and 600 nm making these blends appear olive green with color coordinates between those of lens 1 and lens 3. As with the Orange–Periwinkle blend, this blend also becomes highly transmissive and color neutral ( $L^* 87$ ,  $a^* -3$ ,  $b^* -3$ ) upon oxidation (average  $\Delta\%T$  60%; Figure S8B, Supporting Information). The Yellow–Periwinkle blend is a more muted brown than the Orange–Periwinkle blend, possessing an  $S_{ab}$  of 26 in the colored state.

The low  $a^*$  of the Yellow–Periwinkle blend can be tuned by adding ECP–Orange and making a three component blend. An example of a Yellow–Orange–Periwinkle blend (1.3:1:1) is shown in Figure 3C. The addition of ECP–Orange increases the  $a^*$  from 3 to 15 and the  $b^*$  from 15 to 30, giving a color that is a close match to lens 4 and a higher  $S_{ab}$  of 47. The average  $\Delta\%T$  (Figure S8C, Supporting Information) is 64% at  $\lambda_{max}$  where the improved  $\Delta\%T$  compared to the Yellow–Periwinkle blend is likely to be due to the lower ECP–Yellow content. In the colorless state, the blend has color coordinates of  $L^* 87$ ,  $a^*$

$-0.9$ ,  $b^* -2.5$ , making it the most achromatic of all of the blends.

The final blend presented is a 1:1 Cyan–Orange blend. Using the D50 illuminant this blend has similar color coordinates ( $L^* 65$ ,  $a^* 12$ ,  $b^* 35$ ) when compared to the three-component blend, even though the absorbance spectra of the two blends are remarkably different. This is a result of how a color stimulus is produced by the human eye, where different combinations of light can produce an equivalent receptor response and the same tristimulus values, making two colors with different absorbance spectra appear indistinguishable under a specific illuminant.<sup>32</sup> It is worth noting that the low energy band in this blend is mainly found outside the visible wavelength range (430–730 nm). The  $\Delta\%T$  of a Cyan–Orange blend is 60% at  $\lambda_{max}$  (Figure S8D, Supporting Information) and the color saturation is 50 in the colored state making it the blend with the highest color saturation. The transmissive state for this blend is also highly achromatic with color coordinates of  $L^* 85$ ,  $a^* -2$ ,  $b^* -3$ .

#### Color Evolution and Switching Speeds of ECP Blends.

For more sensitive eyewear applications, the ECP blends would ideally switch between a colored brown state and an achromatic transmissive state without any intermediate color. The onsets of oxidation for the individual ECPs play an important role in affecting this property. Figures 4A and 4C shows the evolution of color as a function of applied voltage for the 1.5:1 Orange–Periwinkle blend and the 1:1 Orange–Cyan blend. Corresponding plots for the other two blends (Yellow–Periwinkle and Yellow–Orange–Periwinkle) are shown in Figure S9 (Supporting Information). The full spectroelectrochemical

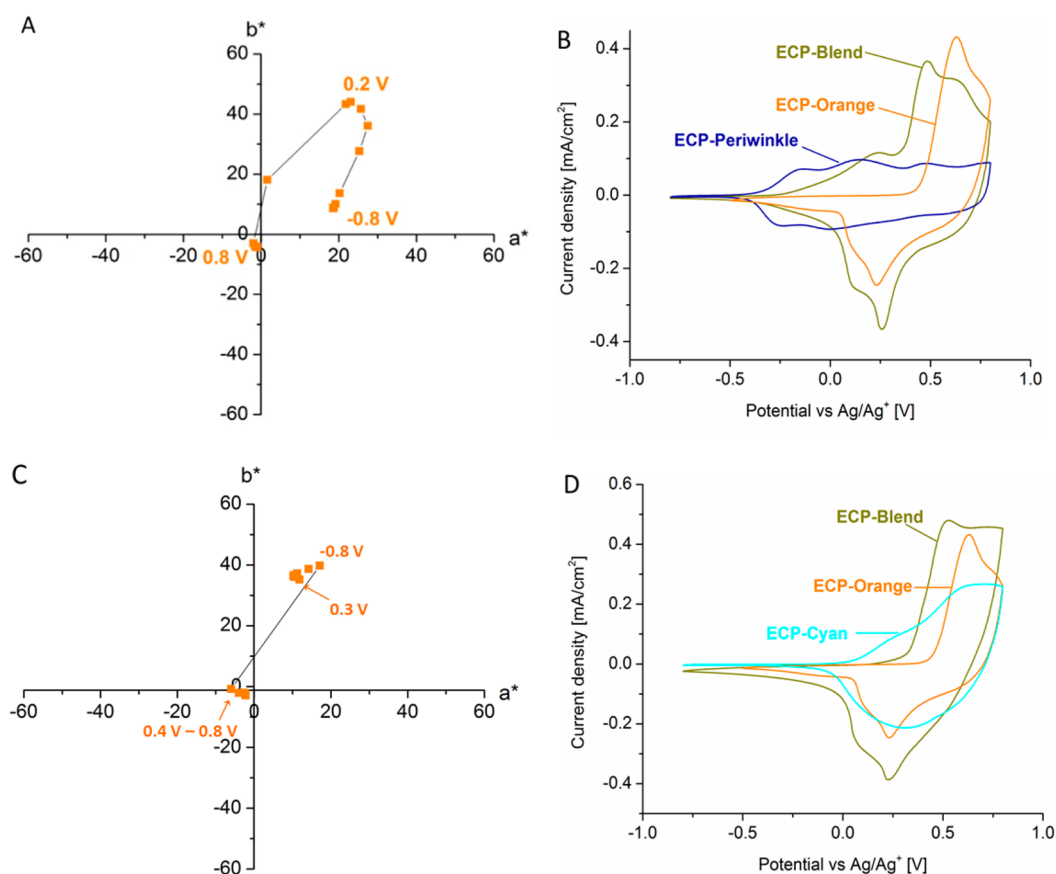


**Figure 4.** Color evolution and cyclic voltammograms of (A and B) the 1.5:1 Orange–Periwinkle blend and (C and D) the 1:1 Orange–Cyan blend on ITO/glass in 0.5 M TBAPF<sub>6</sub>-PC.

characterization of all blends is shown in Figure S10 (Supporting Information). As shown in Figure 4A and Figure S10A (Supporting Information), when the Orange–Periwinkle blend is switched from its neutral state to its fully oxidized state, the color of the blend proceeds through an intermediate orange state between  $-0.2$  and  $0.4$  V before reaching a fully achromatic bleached state at higher potentials. This can be rationalized by looking at the component CVs in Figure 4B where the onset of oxidation for ECP-Periwinkle is  $-0.3$  V, while the onset of oxidation for ECP-Orange does not occur until  $0.4$  V. When the two are blended together, however, the onset for the periwinkle component shifts anodically to  $-0.2$  V, and the onset for the orange component shifts cathodically by approximately the same magnitude. We attribute this to the possibility that ECP-Periwinkle and ECP-Orange phase separate into small domains in intimate contact with each other. At potentials where ECP-Periwinkle normally begins to oxidize, the surrounding ECP-Orange acts as an insulator making the periwinkle component more difficult to oxidize. Once ECP-Periwinkle begins to oxidize, however, ECP-Orange becomes surrounded by conducting material (and ECP-Periwinkle essentially becomes an extension of the electrode), resulting in a lowering of the oxidation potential of the ECP-Orange component in the blend. The same phenomenon and color evolution is found for the Yellow–Periwinkle blend (Figure S9A, Supporting Information) and the Yellow–Orange–Periwinkle blend (Figure S9B, Supporting Information). In contrast, ECP-Cyan and ECP-Orange have closer oxidation potentials and as a result the blend does not have a colored intermediate state, instead proceeding directly from a

brown colored state to a transmissive state, as illustrated in Figure 4C. The slight decrease in both  $a^*$  and  $b^*$  between  $0.1$  and  $0.4$  V is a result of the slightly lower oxidation potential for ECP-Cyan (this is more evident in Figure S10B, Supporting Information); however, this slight change in color is barely visible to the eye. In spite of these observations, it is important to note that these are steady state measurements at discrete voltages. During device operation, the voltage is switched only between two extremes (e.g.,  $-1$  V/ $+1$  V), rather than being held at intermediate voltages, making any intermediate coloration less noticeable if rapidly switching blends are used. However, this illustrates the importance of considering the electrochemistry of each component when designing blends, especially if one or both blend components take a few seconds to fully switch between states.

For ECP blends to be competitive and applicable for advanced eyewear and a broader range of applications, such as flexible displays, they should switch between their colored and highly transmissive states on the order of seconds. As shown in Figure S7 (Supporting Information), when using a three-electrode configuration with a coiled Pt wire counter electrode, the individual components ECP-Periwinkle, ECP-Yellow, and ECP-Cyan switch from the colored to the transmissive state in less than 1 s, while ECP-Orange exhibits slower kinetics, requiring around 5 s to fully oxidize.<sup>23</sup> Interestingly, the switching times of the individual ECP components do not correlate directly with the switching speeds of the blends, as shown in Table 3. In the case of the Orange–Periwinkle film, the blend achieves a full switch in less time than the individual components, while in the case of the Yellow–Periwinkle film,

**Table 3. Transmittance Change and Switching Times for the Brown Blends**

ECP-blend	$\Delta\%T_{100\%}$ <sup>a</sup>	$t_{\text{colorless}}$ <sup>b</sup>	$t_{\text{colored}}$ <sup>c</sup>
orange–periwinkle	68	2.5	1
yellow–periwinkle	60	3.5	2.5
yellow–orange–periwinkle	64	5.5	1
orange–cyan	60	5	7

<sup>a</sup>Change in transmittance at  $\lambda_{\text{max}}$  for a full switch measured at steady state. <sup>b</sup>Time (sec) to reach 90% of full switch upon oxidation, colored-to-colorless transition. <sup>c</sup>Time (sec) to reach 90% of full switch upon reduction, colorless-to-colored transition.

the blend takes longer to switch than its components. This could be related to differences in redox behavior of the blend compared to the components, as discussed in the previous section in conjunction with Figure 4. The blends all display changes in transmittance of 60% or greater at  $\lambda_{\text{max}}$  and switching times on the order of seconds. These switching times are significantly faster than photochromic lenses, especially when switching from the colored state to the colorless state, where photochromic bleaching generally occurs on the order of minutes. While the Orange–Cyan blend shows the slowest transition from the colorless to the colored states, the lack of intermediate coloration as discussed above makes the transition proceed seamlessly between the two states. As seen in Figure 4 and Figure S9 (Supporting Information), the other three blends proceed through intermediate colored states during potential stepping. Of these three blends, the Orange–Periwinkle film attained both the highest change in transmittance and the fastest switching speeds, where the fast switching time compensates for this intermediate coloration. Due to its high performance, we selected this blend to be further investigated in a prototype electrochromic lens.

**Electrochromic Brown Lenses.** Standard sunglasses for regular outdoor use have 15–25% transmittance in the colored state, while sunglasses for more specialized activities, especially those related to winter sports, can require darker lenses with a transmittance as low as 3–5%.<sup>33</sup> Hence, we set out to make a lens with a 5% transmittance in the colored state and evaluate its switching behavior. Using the brown blend with the highest  $\Delta\%T$  and fastest switching time (1.5:1 Orange–Periwinkle), electrochromic lenses were fabricated using a combination of inkjet printing for patterning Ag contacts and blade coating for depositing the ECP and MCCP layers, to demonstrate the performance of the blend in a device using a roll-to-roll compatible coating methods. As evidenced by the photographs in Figure 5, the film quality is smooth and even and possesses

minimal haze over the entire 25 cm<sup>2</sup> surface area in both the colored and colorless states. In the colorless state, objects appear clearly behind the lens, and the colorlessness can be qualitatively assessed by comparing the similarities in the skin tone behind the lens with the skin tone around the lens. From the user's perspective, the lens is sufficiently dark in the colored state to serve as sunglasses, whereas the colorless state has no noticeable color or haze. These properties can be quantifiably observed in the spectra in Figure 6. In the colored state, the spectra ( $L^* 45$ ,  $a^* 18$ ,  $b^* 10$ ) closely resemble those of the film (Figure 3A). In the colorless state, the relatively flat spectrum imparts little coloration to the lens ( $L^* 75$ ,  $a^* 2$ ,  $b^* 2$ ), and the entire lens (including the optical properties from the substrate and the electrolyte as measurements were made versus air) displays a 45%  $\Delta T$  at ( $\lambda_{\text{max}}$ ), with much of the absorbance (20–30%) in this state coming from the ITO/PET foil and the UV-curable electrolyte. Due to the low conductivity of most solid state electrolytes, the device kinetics were expected to be slower than observed for the film switched in an electrolyte solution. However, when switching the lens between  $\pm 1.0$  V using, for example, a small coin-cell battery, the lens switching occurs in less than a second, faster than the Orange–Periwinkle film switched in a three-electrode setup. This enhancement in switching speed is likely due to the increased size and capacitance of the counter electrode (MCCP/ITO/PET) and decreased distance between the two electrodes (ca. 200  $\mu\text{m}$ ) in a device compared with in a three-electrode setup. Because of the rapid device kinetics, the intermediate color state discussed in conjunction to Figure 4A is unnoticeable. These results demonstrate that not only are the colorimetric properties of the brown film preserved when incorporated into a device, but the kinetics may actually be enhanced by more a favorable electrode configuration in a device architecture.

## CONCLUSIONS

The brown hues created in this study demonstrate how fine-tuning of coloration can be achieved in a straightforward fashion through color mixing of soluble electrochromic polymers without having to devise synthetic routes. This provides access to a wide spectrum of colors without the need to synthesize each individual hue, but rather with only a handful of starting ECP components. The blends all displayed switching times between colored and colorless states on the order of seconds, with changes in transmittance of 60–68%. Interestingly, the redox potentials of the components shifted when the components were blended together, and the switching speeds improved for one blend, suggesting that the interaction

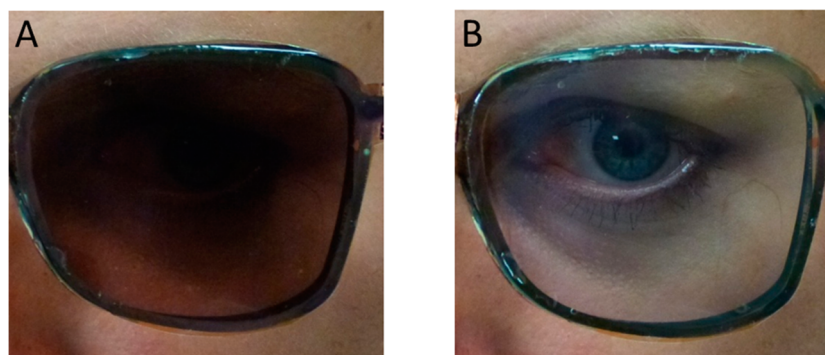


**Figure 5.** Photographs of the electrochromic lens at (A)  $-1.0$  V ( $L^* 45$ ,  $a^* 18$ ,  $b^* 10$ ) and (B) at  $+1.0$  V ( $L^* 75$ ,  $a^* 2$ ,  $b^* 2$ ).

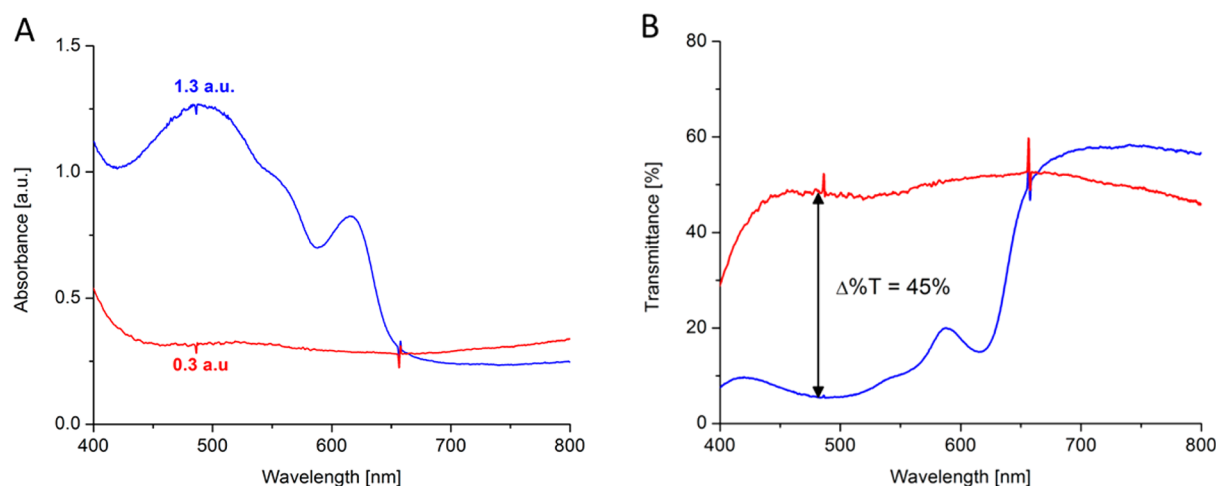


**Figure 6.** (A) Absorbance spectra and (B) transmittance spectra of the electrochromic lens in the colored (blue line) and the colorless states (red line).

between the polymer components is complex and worth further study. The highest performance blend was incorporated into a solid-state lens prototype with an MCCP counter electrode, where the entire device was assembled using roll-to-roll compatible techniques. The lens achieved highly transmissive colored and colorless states with fast switching in a  $\pm 1$  V window and a 45% change in transmittance upon a full switch (not subtracting the contributions from the electrolyte and the substrate). The more rapid switching speed of the lens relative to the films results, likely due to the larger surface area and closer placement of the counter electrode, making the lens configuration an ideal device architecture for electrochromic applications. The rapid switching kinetics also made the intermediate coloration unnoticeable in the lens. These results demonstrate the competitiveness of blended ECPs, from both an aesthetic and a performance-related standpoint, for user-controlled electrochromic eyewear applications.

## ■ ASSOCIATED CONTENT

### 📄 Supporting Information

Detailed syntheses of ECP-Yellow and ECP-Periwinkle, switching kinetics for ECP components, colorimetric data, transmittance spectra, and spectroelectrochemical characterization of the brown blends. This material is available free of charge via the Internet at <http://pubs.acs.org>.

## ■ AUTHOR INFORMATION

### Corresponding Authors

\* E-mail: [anna.osterholm@chemistry.gatech.edu](mailto:anna.osterholm@chemistry.gatech.edu).

\* E-mail: [reynolds@chemistry.gatech.edu](mailto:reynolds@chemistry.gatech.edu).

### Author Contributions

A.M.Ö. designed and characterized all ECP-blends and fabricated and tested the electrochromic lenses; D.E.S. designed, fabricated, and tested the electrochromic lenses; J.A.K. synthesized and characterized ECP-Orange and ECP-Periwinkle and designed ECP-Yellow; M.K. carried out the syntheses of bithiophene, ECP-Cyan, and ECP-Yellow; R.H.B. and A.L.D. contributed to data analysis; A.M.Ö., D.E.S., and J.R.R. wrote the manuscript. All authors have given approval to the final version of the manuscript.

### Notes

The authors declare no competing financial interest.

## ■ ACKNOWLEDGMENTS

We thank BASF for financial support and Kai Sudau for assistance with inkjet printing and lens design.

## ■ REFERENCES

- (1) Transitions Home Page. [www.transitions.com](http://www.transitions.com) (accessed October 2014).
- (2) Rudy Project ImpactX Lenses. [www.rudyprojectusa.com](http://www.rudyprojectusa.com) (accessed October 2014).
- (3) 3M Smart Lens Protective Eyewear. [www.solutions.3m.com](http://www.solutions.3m.com) (accessed October 2014).
- (4) Honeywell Uvex Milan Safety Eyewear. [www.honeywellsafety.com](http://www.honeywellsafety.com) (accessed October 2014).
- (5) Dyer, A. L.; Thompson, E. J.; Reynolds, J. R. Completing the Color Palette with Spray-Processable Polymer Electrochromics. *ACS Appl. Mater. Interfaces* **2011**, *3*, 1787–1795 and references therein.
- (6) Shi, P.; Amb, C. M.; Knott, E. P.; Thompson, E. J.; Liu, D. Y.; Mei, J.; Dyer, A. L.; Reynolds, J. R. Broadly Absorbing Black to Transmissive Switching Electrochromic Polymers. *Adv. Mater.* **2010**, *22*, 4949–4953.
- (7) Beaujuge, P. M.; Ellinger, S.; Reynolds, J. R. The Donor–Acceptor Approach Allows a Black-to-Transmissive Switching Polymeric Electrochromic. *Nat. Mater.* **2008**, *7*, 795–799.
- (8) Kim, Y.; Kim, H.; Graham, S.; Dyer, A.; Reynolds, J. R. Durable Polyisobutylene Edge Sealants for Organic Electronics and Electrochemical Devices. *Sol. Energy Mater. Sol. Cells* **2012**, *100*, 120–125.
- (9) Jensen, J.; Madsen, M. V.; Krebs, F. C. Photochemical Stability of Electrochromic Polymers and Devices. *J. Mater. Chem. C* **2013**, *1*, 4826–4835.
- (10) Chandrasekhar, P.; Zay, B. J.; Cai, C.; Chai, Y.; Lawrence, D. Matched-Dual-Polymer Electrochromic Lenses, Using New Cathodically Coloring Conducting Polymers with Exceptional Performance and Incorporated Into Automated Sunglasses. *J. Appl. Polym. Sci.* **2014**, *131*, 41043.
- (11) Ma, C.; Taya, M.; Xu, C. Smart Sunglasses Based on Electrochromic Polymers. *Polym. Eng. Sci.* **2008**, *48*, 2224–2228.
- (12) Ma, C.; Zheng, J.; Yang, S.; Zhu, D.; Bin, Y.; Xu, C. Electrochromic Kinetics of Nanostructured Poly(3,4-(2,2-dimethylpropylenedioxy)thiophene) Film on Plastic Substrate. *Org. Electron.* **2011**, *12*, 980–987.
- (13) Dyer, A. L.; Bulloch, R. H.; Zhou, Y.; Kippelen, B.; Reynolds, J. R.; Zhang, F. A Vertically Integrated Solar-Powered Electrochromic Window for Energy Efficient Buildings. *Adv. Mater.* **2014**, *26*, 4895–4900.
- (14) Amasawa, E.; Sagasawa, N.; Kimura, M.; Taya, M. Design of a New Energy-Harvesting Electrochromic Window Based on an Organic



Polymeric Dye, a Cobalt Couple, and PProDOT-Me<sub>2</sub>. *Adv. Energy Mater.* **2014**, *4*, 1400379.

(15) Kumar, A.; Otley, M. T.; Alamar, F. A.; Zhu, Y.; Arden, B. G.; Sotzing, G. A. Solid-State Electrochromic Devices: Relationship of Contrast as a Function of Device Preparation Parameters. *J. Mater. Chem. C* **2014**, *2*, 2510–2516.

(16) Jensen, J.; Krebs, F. C. From the Bottom Up—Flexible Solid State Electrochromic Devices. *Adv. Mater.* **2014**, *26*, 7231–7234.

(17) Beaupre, S.; Breton, A.-C.; Dumas, J.; Leclerc, M. Multicolored Electrochromic Cells Based on Poly(2,7-carbazole) Derivatives for Adaptive Camouflage. *Chem. Mater.* **2009**, *21*, 1504–1513.

(18) Bulloch, R. H.; Kerszulis, J. A.; Dyer, A. L.; Reynolds, J. R. Mapping the Broad CMY Subtractive Primary Color Gamut Using a Dual-Active Electrochromic Device. *ACS Appl. Mater. Interfaces* **2014**, *6*, 6623–6630.

(19) Ersman, P. A.; Kawahara, J.; Berggren, M. Printed Passive Matrix Addressed Electrochromic Displays. *Org. Electron.* **2013**, *14*, 3371–3378.

(20) Ashwin-Ushas Home Page. <http://www.ashwin-ushas.com> (accessed October 2014).

(21) Amb, C. M.; Dyer, A. L.; Reynolds, J. R. Navigating the Color Palette of Solution-Processable Electrochromic Polymers. *Chem. Mater.* **2011**, *23*, 397–415.

(22) Beaujuge, P. M.; Reynolds, J. R. Color Control in  $\pi$ -Conjugated Organic Polymers for Use in Electrochromic Devices. *Chem. Rev.* **2010**, *110*, 268–320.

(23) Dyer, A. L.; Craig, M. R.; Babiarz, J. E.; Kayak, K.; Reynolds, J. R. Orange and Red to Transmissive Electrochromic Polymers Based on Electron-Rich Dioxathiophenes. *Macromolecules* **2010**, *43*, 4460–4467.

(24) Estrada, L. A.; Deininger, J. J.; Kamenov, G. D.; Reynolds, J. R. Direct (Hetero)arylation Polymerization: An Effective Route to 3,4-Propylenedioxythiophene-Based Polymers with Low Residual Metal Content. *ACS Macro Lett.* **2013**, *2*, 869–873.

(25) Reeves, B. D.; Grenier, C. R. G.; Argun, A. A.; Cirpan, A.; McCarley, T. D.; Reynolds, J. R. Spray Coatable Electrochromic Dioxathiophene Polymers with High Coloration Efficiencies. *Macromolecules* **2004**, *37*, 7559–7569.

(26) CIE 15: Technical Report: Colorimetry. Commission Internationale de L'éclairage: Vienna, Austria, 2004.

(27) Knott, E. P.; Craig, M. R.; Liu, D. Y.; Babiarz, J. E.; Dyer, A. L.; Reynolds, J. R. A Minimally Coloured Dioxypyrrole Polymer as a Counter Electrode Material in Polymeric Electrochromic Window Devices. *J. Mater. Chem.* **2012**, *22*, 4953–4962.

(28) Amb, C. M.; Kerszulis, J. A.; Thompson, E. J.; Dyer, A. L.; Reynolds, J. R. Propylenedioxythiophene (ProDOT)-Phenylene Copolymers Allow a Yellow-to-Transmissive Electrochrome. *Polym. Chem.* **2011**, *2*, 812–814.

(29) Kerszulis, J. A.; Amb, C. M.; Dyer, A. L.; Reynolds, J. R. Follow the Yellow Brick Road: Structural Optimization of Vibrant Yellow-to-Transmissive Electrochromic Conjugated Polymers. *Macromolecules* **2014**, *47*, 5462–5469.

(30) Thompson, B. C.; Kim, Y.-G.; McCarley, T. D.; Reynolds, J. R. Soluble Narrow Band Gap and Blue Propylenedioxythiophene–Cyanovinylene Polymers as Multifunctional Materials for Photovoltaic and Electrochromic Applications. *J. Am. Chem. Soc.* **2006**, *128*, 12714–12725.

(31) Amb, C. M.; Beaujuge, P. M.; Reynolds, J. R. Spray-Processable Blue-to-Highly Transmissive Switching Polymer Electrochromes via the Donor–Acceptor Approach. *Adv. Mater.* **2010**, *22*, 724–728.

(32) Wyszecki, G.; Stiles, W. S. *Color Science: Concepts and Methods, Quantitative Data and Formulae*; John Wiley & Sons: New York, 2000.

(33) Ophthalmic Lens Tints and Coatings. <http://www.eyecalcs.com/DWAN/pages/v1/v1c051d.html> (accessed October 2014).